Available online at www.sciencedirect.com
SCIENCE DIRECT®
Journal of Power Sources 119–121 (2003) 658–663
JOURNAL OF POWER SOURCES
www.elsevier.com/locate/jpowsour

Electroanalytical and thermal stability studies of multi-doped lithium nickel cobalt oxides

G.T.K. Fey*, J.G. Chen, V. Subramanian

Department of Chemical and Materials Engineering, National Central University, Chung-Li 320 54, Taiwan, ROC

Abstract

Lithiated nickel cobalt oxides are intensively being investigated for possible application in lithium batteries. Improving their electrochemical properties and thermal stability will enhance their chances for commercial application. In the present study, we report the electroanalytical and thermal properties of $LiNi_{0.7}Co_{0.2}Ti_{0.05}M_{0.05}O_2$ (M = Al, Mg, Zn). Cyclic voltammetry experiments revealed the reversibility of the lithium intercalation processes. Impedance measurements showed a decrease in the charge transfer resistance as lithium extraction progressed. The Mg-doped system showed the best cyclability over 100 cycles, followed closely by the Al-doped system. Mg as a dopant led to improved thermal stability of the cathode material in the fully charged state. However, doping with Al or Zn resulted in reduced thermal stability.

Keywords: Layered oxides; Lithium nickel cobalt oxides; Thermal stability; Impedance; Spectroscopy; Lithium-ion battery

1. Introduction

Solid solutions of the general formula $LiNi_{1-y}Co_yO_2$ ($0.2 \leq y \leq 0.4$), by virtue of the minimal changes in their unit cell volumes during cycling [1,2] and high-rate capability [3], have attracted considerable interest recently. Efforts to improve their electrochemical properties and thermal stability have also been under close scrutiny [4,5]. Doping with multiple ions in $LiNi_{1-y}Co_yO_2$ solid solutions, especially in the nickel-rich regions ($y = 0.1$–0.3), has been shown to improve cyclability and thermal stability [6]. Recently, Lee et al. [7] reported that doping with Fe or Al for Ni in $LiNi_{0.85}Co_{0.15}O_2$ resulted in improved stability with respect to cycling. Similarly, Mg-doped $LiNi_{1-y}Co_yO_2$ has also been shown to exhibit good cyclability and safety characteristics [8]. In general, doping with non-transition metal ions leads to improved safety and cycling stability for the $LiNi_{1-y}Co_yO_2$ system. Al and Mg have been extensively studied as dopants, but doping with other non-transition metals such as Zn has not been studied in detail. We recently reported our preliminary results on the synthesis and electrochemical properties of Al-, Mg- or Zn-doped $LiNi_{0.85}Co_{0.20}O_2$ systems [9]. Ti as a dopant in $LiNiO_2$ and related structures has been pursued by several groups. Ti as a single dopant [10] or as a co-dopant with Mg [11,12] has been shown to impart desirable stabilizing effects by suppressing phase transformation during cycling.

Understanding the electrochemical characteristics of materials used in lithium batteries will help improve lithium battery performance. Levi et al. [13–15] have done pioneering work on the electroanalytical behavior of lithium battery electrode materials using techniques such as EIS, SSCV, PITT and GITT. In this paper, we report results from a study on the cycling performance, electrode kinetics and thermal stability of $LiNi_{0.7}Co_{0.2}Ti_{0.05}M_{0.05}O_2$ (M = Al, Mg, Zn).

2. Experimental

The multi-doped compounds were prepared by a conventional solid-state method, details of which are given elsewhere [9]. The structural and morphological characterizations have also been reported [9].

Electrochemical studies were performed on 2032-type coin cells with a lithium metal anode. The electrolyte was a 1 M solution of $LiPF_6$ in a 50:50 (v/v) mixture of EC/DEC (Tomiyama Chemicals). The fabrication of the cathodes and cell assembly are described elsewhere [9]. Electrochemical cycling was performed in the galvanostatic mode at a 0.1 C rate between 2.5 and 4.3 V in a multi-channel battery cycling unit (Maccor, Series 4000). Cyclic voltammetric measurements were done by a Solartron 1287 electrochemical interface between 2.5 and 4.4 V at a scan rate of 100 μV/s. Details of cell construction for cyclic voltammetric studies are

* Corresponding author. Tel.: +886-3-422-7151-4206; fax: +886-3-425-7325.
E-mail address: gfey@cc.ncu.edu.tw (G.T.K. Fey).

0378-7753/03/$ – see front matter
doi:10.1016/S0378-7753(03)00201-5

described elsewhere [16]. Electrochemical impedance spectra at different depths of charge and discharge were recorded for the coin cells on a Solartron 1250/1287 set up between 65 kHz and 0.001 Hz.

Thermal characterization of the multi-doped $LiNi_{0.8}Co_{0.2}O_2$ was done on a Perkin-Elmer DSC 7 differential scanning calorimeter. The measurements were made in N_2 atmosphere between 150 and 350 °C at a heating rate of 3 °C/min. The samples for the DSC experiments were prepared as follows. The coin cells were first galvanostatically charged to 4.4 V at a 0.1 C rate and then potentiostated at 4.4 V for 20 h. During this period, the current dropped to microampere levels. After 20 h, the coin cells were opened inside a glove box. The cathode of the coin cell was carefully removed and the excess electrolyte was wiped with a Kimwipes® cloth. All the recovered materials had 10–15% electrolyte by weight. The material was carefully scrapped from the aluminum current collector and loaded on to an aluminum pan. The aluminum pan was hermetically sealed, placed in an airtight container, and immediately transferred to the DSC instrument.

3. Results and discussion

3.1. Cyclic voltammetric studies

Cyclic voltammograms recorded for the three non-transition metal ion-doped systems are shown in Fig. 1. Since the only variants in the materials are the non-transition metal ions, any differences in performance characteristics between the three systems must arise only from the dopants. There appear to be no irreversible oxidation peaks that can be associated with electrolyte decomposition. The main oxidation peak appears ca. 4.0 V, with its corresponding reduction peak ca. 3.7 V. In addition to the redox peaks, unsubstituted $LiNiO_2$ has been shown to exhibit several peaks at higher potentials corresponding to the progressive transformation from the hexagonal (H1) phase to the monoclinic (M) to the hexagonal (H2) to the hexagonal (H3) phases, where the H's represent phases with hexagonal symmetry, but different lattice parameters [4,17–21]. According to Levi et al. [13], when the cell voltage approaches 4.15 V, lithium concentration increases in the hexagonal phase. When the voltage crosses above 4.20 V, two hexagonal co-existing phases appear [13]. The non-transition metal ions are believed to shift the oxidation voltage well above that for the undoped $LiNi_{0.8}Co_{0.2}O_2$ system [13]. The hexagonal-to-monoclinic phase transformation is a major cause of structural degradation [22].

In the case of the Mg-doped material, no additional peaks that may suggest phase transformations could be observed. Thus, the incorporation of Mg in $LiTi_{0.05}Ni_{0.75}Co_{0.2}O_2$ suppresses phase transformations at the high potentials. Chang et al. [23], who studied the effect of Mg doping in $LiNiO_2$, reported a similar suppression of such peaks in the

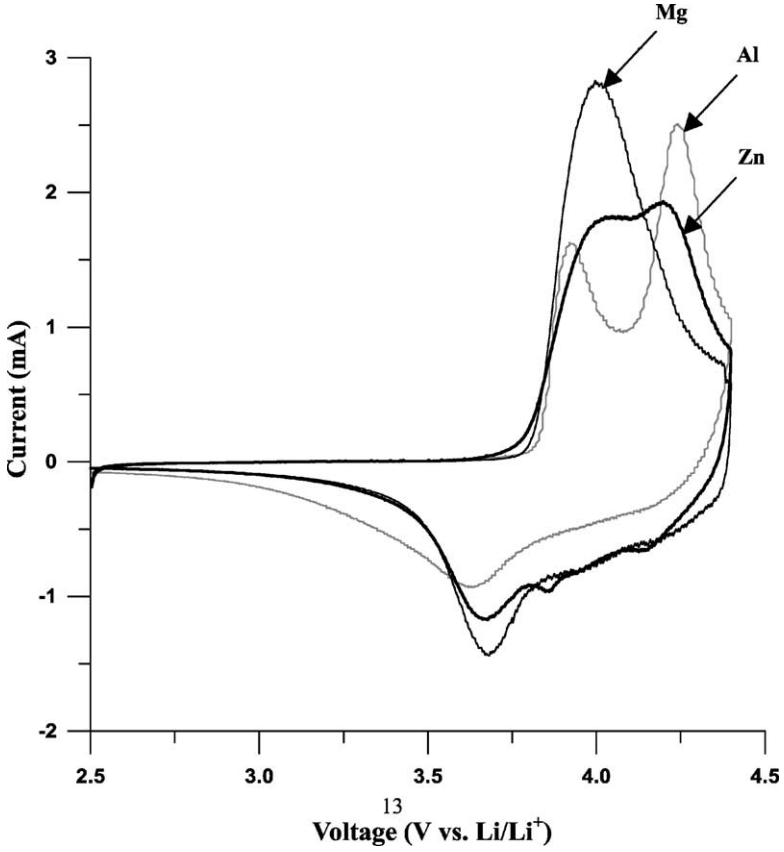

Fig. 1. Cyclic voltammograms of $LiNi_{0.7}Co_{0.2}Ti_{0.05}M_{0.05}O_2$ (M = Mg, Al or Zn).

doped compounds. The authors [23] suggested that Mg occupied Ni sites in the $LiNiO_2$ lattice, preventing a Li-vacancy ordering that is reported to cause phase transformations [24]. Similar results have been reported by Yu et al. [25] in their studies with $LiGa_{0.02}Mg_{0.03}Ni_{0.95}O_2$. The reduction peak was not as well defined as the oxidation peak for the Mg-doped material because of the formation of a passivation layer upon charging as well as modification of the electronic structure of the system [26]. Both the Al- and the Zn-doped materials exhibited high-potential peaks suggestive of phase transformations, although the profiles appeared very depressed in the case of the latter. Cho et al. [27] observed similar cyclic voltammetric profiles for Al_2O_3-coated $LiCoO_2$. Also, the integrated area of the peaks in the cyclic voltammogram for the Zn-doped system was comparatively lower than those for the other two systems. In other words, the currents associated with the oxidation and reduction reactions of the Zn-doped system were comparatively lower.

3.2. Charge–discharge studies—long cycle performance

The cycling data for 40 cycles at a charge–discharge rate of 0.1 C between 2.5 and 4.3 V show that $LiNi_{0.8}Co_{0.2}O_2$ delivered a discharge capacity of 174 mAh/g in the first cycle, which faded to 134 mAh/g in the 40th cycle. In the case of $LiTi_{0.05}Ni_{0.75}Co_{0.2}O_2$, the first cycle capacity was only 159 mAh/g. However, the capacity in the 40th cycle was higher at 142 mAh/g. It should be noted that Ti doping in $LiNi_{0.8}Co_{0.2}O_2$ enhanced the capacity retention from 77.0 to 89.3% over 40 cycles. Al, Mg and Zn as co-dopants reduced first cycle capacities to 153, 145 and 140 mAh/g, respectively. However, the capacities recorded in the 40th cycle were 142, 139 and 126 mAh/g, respectively, which are higher than those of $LiNi_{0.8}Co_{0.2}O_2$ and $LiTi_{0.05}Ni_{0.75}Co_{0.2}O_2$. The capacity retention over 40 cycles jumped to 92.8, 95.9, and 91.4% for the Al-, Mg-, and Zn-doped $LiNi_{0.8}Co_{0.2}O_2$, respectively. Thus, although the co-dopants may reduce the initial capacity, they enhance the cyclability of the system.

According to Van der Ven and Ceder [28], the electrochemical properties of the O3-layered structure depend on how easily lithium can diffuse in the structure. Therefore, it appears that the Al- and Zn-doped systems have increased levels of cation mixing, which lead to their poor electrochemical performance. Apparently, the cation mixing was comparatively lower for the Al-doped system than for the Zn-doped system [9]. Support for this argument comes from the poor electrochemical behavior of the Zn-doped system. The maximum cycling stability of the Mg-doped system, as reflected by its lowest capacity fade, is attributed to the low levels of cation mixing in these systems [9]. Small concentrations of dopant ions in the lithium plane can act as pillars that provide extra structural stability to the system, resulting in enhanced cyclability. Additionally, Mg occupancy in Ni sites helps retain more Li in the charged state and stabilizes the NiO slabs [23], resulting in an increase in cyclability.

Extended cycling of the doped systems shows that the Mg-doped compound delivered 132 mAh/g in the 100th cycle, with a charge retention value of 91.0%. The Al-doped system faded faster, giving only 129 mAh/g in the 100th cycle and registering a charge retention of 84.3%. In comparison, the capacity of the Zn-doped compound was only 115 mAh/g in the 100th cycle (capacity retention: 82.1%). Cycling behavior of the co-doped compounds is compared with the behavior of the undoped compounds in Fig. 2.

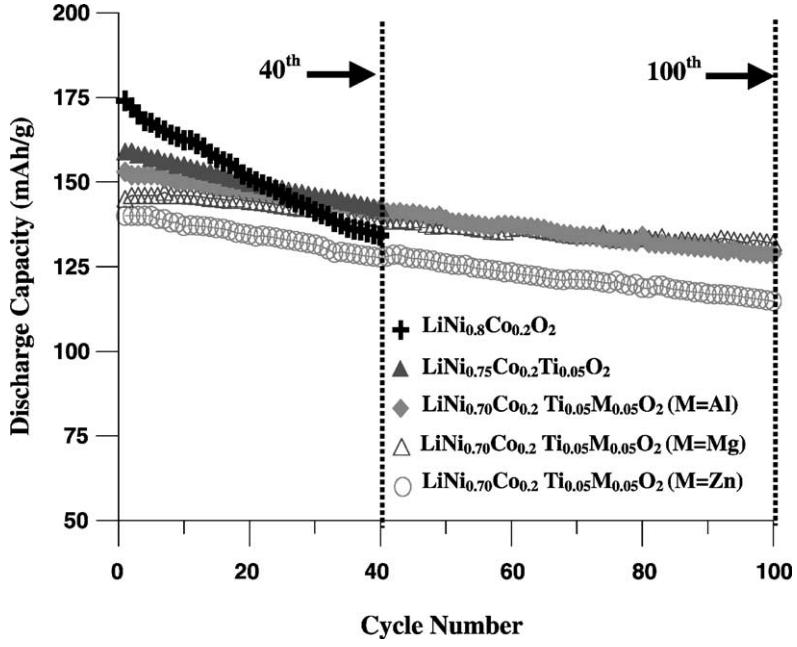

Fig. 2. Long-cycling behavior of the various $LiNi_{0.7}Co_{0.2}Ti_{0.05}M_{0.05}O_2$ (M = Mg, Al or Zn) compositions.

3.3. Thermal stability studies

Lithiated nickel oxide-based cathode materials are associated with great safety concern as they enter into an exothermic decomposition reaction with the electrolyte in the fully charged state at elevated temperatures. The partial substitution of Ni by Co in $LiNiO_2$ not only helps suppress this exothermic reaction, but also shifts the reaction to a higher temperature. A study of the exothermic decomposition of the doped and undoped systems would help explain the effect of the dopant ions on the thermal stability of the oxide material. The thermal behavior of the fully charged $LiNi_{0.7}Co_{0.2}Ti_{0.05}M_{0.05}O_2$ samples is summarized in Table 1.

The exothermic decomposition of $LiTi_{0.05}Ni_{0.75}Co_{0.2}O_2$ was found to occur at 221 °C, the heat of reaction being 62.0 J/g (Table 1). The exothermic reaction is attributed to the reaction of the highly oxidizing Ni^{4+} ions with the organic electrolyte, which results in the evolution of flammable gases. In the case of the Mg- and Al-doped systems, the decompositions occurred at 221 and 223 °C, respectively. However, the values of the heat of reaction were 41.4 and 72.9 J/g, respectively. The reduced exothermicity of the reaction of the Mg-doped material indicates its increased

Table 1
Thermal history of the fully charged doped cathode materials studied by DSC

System	Decomposition temperature (°C)	Exothermic enthalpy (J/g)
$LiNi_{0.7}Co_{0.2}Ti_{0.05}Mg_{0.05}O_2$	221	41.4
$LiNi_{0.7}Co_{0.2}Ti_{0.05}Al_{0.05}O_2$	223	72.9
$LiNi_{0.7}Co_{0.2}Ti_{0.05}Zn_{0.05}O_2$	215	78.3
$LiNi_{0.75}Co_{0.2}Ti_{0.05}O_2$	221	62.0

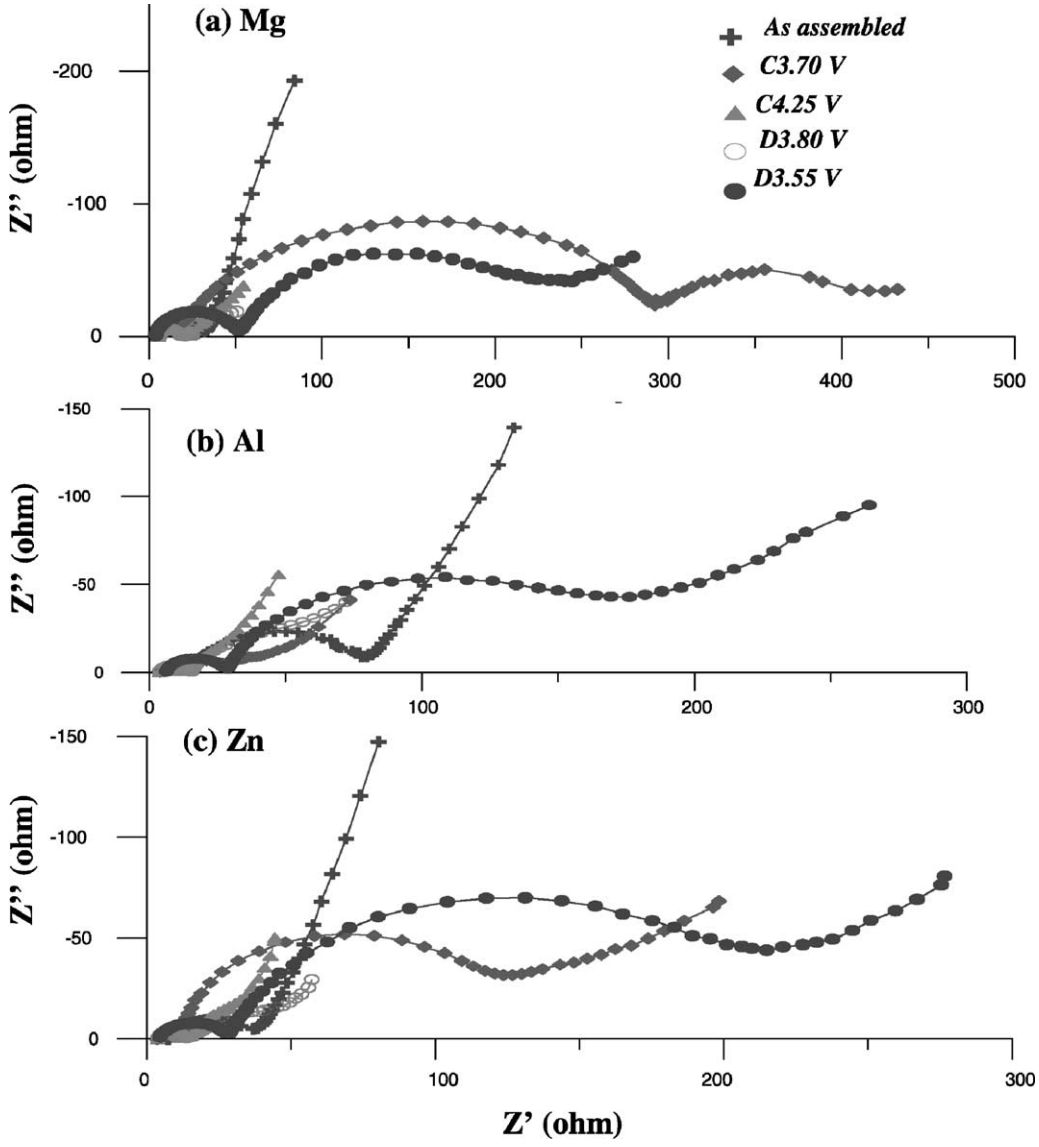

Fig. 3. A family of Nyquist plots recorded for the doped systems at the voltages mentioned in the figure. C and D refer to charge and discharge.

stability. A similar reduction in exothermicity brought about by Mg incorporation was noted by Chang et al. [23] in their studies with $LiMg_{0.15}Ni_{0.85}O_2$. The increased stabilization of the NiO slabs is supposed to prevent the decomposition reaction [23]. However, the apparent increase in the stability of the Al-doped system, reflected by its slightly higher decomposition temperature, is compromised by the higher exothermicity of its decomposition reaction. On the other hand, the reduced decomposition temperature, as well as the higher heat of reaction observed with the Zn-doped material, present a greater thermal hazard for device application. Thus, Mg as a co-dopant bestowed the greatest increase in thermal stability to $LiNi_{0.8}Co_{0.2}O_2$. In a similar study on the simultaneous doping of Mg and Ti in $LiNi_{0.8}Co_{0.2}O_2$, the exothermic decomposition temperature was reported as 221 °C [12].

3.4. Electrochemical impedance spectroscopic studies

Electrochemical impedance spectroscopy aids the understanding of electrode kinetics by analyzing the variation in impedances associated with the different processes during lithium intercalation–deintercalation reactions. Fig. 3 gives a family of Nyquist plots for the different doped systems at various charging and discharging voltages.

The impedance spectrum of the as-assembled cell shows a high-frequency semicircle that indicates a surface film over the oxide, and a low-frequency spike that indicates lithium-ion diffusion in the solid cathode matrix. As lithium ions are removed (charging), a second semicircle in the mid-frequency range emerges (Fig. 3b). The second semicircle is related to the charge transfer phenomenon at the electrode–electrolyte interface. The diameter of this semicircle decreases as the deintercalation progresses. The decrease in the charge transfer resistance with respect to the increased deintercalation of lithium ions is because of an insulator-to-metal transition. Similar observations have been reported by many others [13,14,29,30]. The Warburg tail appearing in all the spectra is due to the diffusion of lithium ions in the oxide electrode.

The impedance parameters associated with the different processes in the three metal ion-doped systems were studied by equivalent circuit modeling. Details of the models used in the present study are given in our earlier communication [16]. Impedance parameters such as the solution resistance, R_s, the particle-to-particle resistance, R_p, the charge transfer resistance, R_{ct}, and the Warburg impedance associated with lithium-ion diffusion were derived. The charge transfer resistance depended on the voltage at which the impedance spectrum was measured. The electrolyte and the particle-to-particle resistances did not show any major dependence on the lithium content or on the voltage at which the impedance measurement was made, a finding which agrees with previously reported results [13,14]. Similarly, the capacitance associated with the surface layer and the charge transfer across the electrode–electrolyte interface were found to be in the order of microfarad (μF) and a few hundred millifarad (mF), respectively, which also agree well with the results already reported [14].

4. Conclusions

Charge–discharge and cyclability, electrochemical impedance, cyclic voltammetry and thermal stability studies were carried out on $LiNi_{0.7}Co_{0.2}Ti_{0.05}M_{0.05}O_2$ (M = Mg, Al or Zn) systems. The Mg-doped system showed the best cyclability over 100 cycles, followed closely by the Al-doped system. The Mg-doped system showed an increase in thermal stability as reflected by its reduced exothermic heat of decomposition as compared to $LiNi_{0.75}Co_{0.2}Ti_{0.05}O_2$. Al and Zn as co-dopants resulted in less thermal stability. Impedance spectroscopic studies showed a decrease in the charge transfer resistance as deintercalaton progressed.

Acknowledgements

The financial support for this work was provided by the National Science Council of the Republic of China, under Contract No. NSC-90-2214-E-008-003. One of the authors (V. Subramanian) thanks the National Science Council for the award of a post-doctoral fellowship.

References

[1] C. Delmas, I. Saadoune, Solid State Ionics 53–56 (1992) 370.
[2] C. Delmas, I. Saadoune, A. Rougier, J. Power Sources 43–44 (1993) 595.
[3] J. Cho, H. Jung, Y. Park, G. Kim, H.S. Lim, J. Electrochem. Soc. 147 (2000) 15.
[4] T. Ohzuku, A. Ueda, M. Kouguchi, J. Electrochem. Soc. 142 (1995) 4033.
[5] E. Rossen, C.D. Jones, J.R. Dahn, Solid State Ionics 57 (1992) 311.
[6] Y. Gao, M. Yakovleva, E. Ebner, A. Quinn, R. Schwindeman, B. Fitch, J. Engel, Electrochem. Soc., Fall Meeting, Boston, USA, 1998.
[7] K.K. Lee, W.S. Yoon, K.B. Kim, K.Y. Lee, S.T. Hong, J. Power Sources 97–98 (2001) 308.
[8] J. Cho, Chem. Mater. 12 (2000) 3089.
[9] V. Subramanian, G.T.K. Fey, Solid State Ionics 148 (2002) 351.
[10] H. Arai, S. Okada, Y. Sakurai, J. Yamaki, J. Electrochem. Soc. 144 (1997) 3117.
[11] Y. Gao, M.V. Yakovleva, W.B. Ebner, Electrochem. Solid-State Lett. 1 (1998) 117.
[12] B.V.R. Chowdari, G.V. Subba Rao, S.Y. Chow, Solid State Ionics 140 (2001) 55.
[13] M.D. Levi, G. Salitra, B. Markovsky, H. Teller, D. Aurbach, U. Heider, L. Heider, J. Electrochem. Soc. 146 (1999) 1279.
[14] M.D. Levi, K. Gamolsky, D. Aurbach, U. Heider, R. Oesten, Electrochim. Acta 45 (2000) 1781.
[15] M.D. Levi, D. Aurbach, J. Phys. Chem. B 101 (1997) 4630.
[16] V. Subramanian, H.S. Chow, C.L. Chen, G.T.K. Fey, J. Mater. Chem. 11 (2001) 3348.

[17] W. Ebner, D. Fouchard, L. Xie, Solid State Ionics 69 (1994) 238.
[18] M. Broussely, F. Penton, P. Biensan, J.M. Bodet, J. Labat, A. Lecerf, C. Delmas, A. Rougier, J.P. Peres, J. Power Sources 54 (1995) 109.
[19] S. Yamada, M. Fujiwara, M. Kanda, J. Power Sources 54 (1995) 209.
[20] H. Arai, S. Okada, H. Ohtsuka, M. Ichimura, J. Yamaki, Solid State Ionics 80 (1995) 261.
[21] H. Arai, S. Okada, Y. Yamada, J. Yamaki, Soild State Ionics 95 (1997) 275.
[22] J. Cho, Y.J. Kim, B. Park, J. Electrochem. Soc. 148 (2001) A1110.
[23] C.C. Chang, J.Y. Kim, P.N. Kumta, J. Electrochem. Soc. 147 (2000) 1722.
[24] J.P. Peres, F. Weill, C. Delmas, Solid State Ionics 116 (1999) 19.
[25] A. Yu, G.V. Subba Rao, B.V.R. Chowdari, Solid State Ionics 135 (2000) 131.
[26] F. Corse, F. Nobili, A. Deptula, W. Lada, R. Tossici, A. D'Epifanio, B. Scrosati, R. Marassi, Electrochem. Commun. 1 (1999) 605.
[27] J. Cho, J.Y. Kim, B. Park, Chem. Mater. 12 (2000) 3788.
[28] A. Van der Ven, G. Ceder, Electrochem. Solid-State Lett. 3 (2000) 301.
[29] F. Nobili, R. Tossici, F. Corce, B. Scrosati, R. Marassi, J. Power Sources 94 (2001) 238.
[30] F. Nobili, F. Corce, B. Scrosati, R. Marassi, Chem. Mater. 13 (2001) 1642.